Molecular Crystals and Liquid Crystals

Publication details, including instructions for authors and subscription information:
http://www.tandfonline.com/loi/gmcl20

Computer Simulation of Pressure-Area Isotherms of Monolayers of Charged Fatty-Acid Molecules

Yehudi K. Levine [a] & Antonino Polimeno [b]

[a] Section for Computational Biophysics, Ornstein Laboratory, Debye Institute, P.O. Box 80.000, Utrecht, 3508 TA, The Netherlands

[b] Dipartimento di Chimica Fisica, Università di Padova, via Loredan 2, Padova, 35131, Italy

Version of record first published: 18 Oct 2010

To cite this article: Yehudi K. Levine & Antonino Polimeno (2003): Computer Simulation of Pressure-Area Isotherms of Monolayers of Charged Fatty-Acid Molecules, Molecular Crystals and Liquid Crystals, 395:1, 193-212

To link to this article: http://dx.doi.org/10.1080/15421400390193774

Mol. Cryst. Liq. Cryst., Vol. 395, pp. [193]/23–[212]/42, 2003

ISSN 1542-1406 print/1563-5287 online
DOI: 10.1080/15421400390193774

Taylor & Francis
Taylor & Francis Group

COMPUTER SIMULATION OF PRESSURE-AREA ISOTHERMS OF MONOLAYERS OF CHARGED FATTY-ACID MOLECULES

Yehudi K. Levine
Debye Institute, Section for Computational Biophysics, Ornstein Laboratory, P.O. Box 80.000, 3508 TA, Utrecht, The Netherlands

Antonino Polimeno
Dipartimento di Chimica Fisica, Università di Padova, via Loredan 2, 35131 Padova, Italy

We present a new Monte Carlo algorithm for simulating the conformational behaviour of surfactant soap molecules tethered to a planar interface. The extension to other geometrical arrangements is straightforward. The algorithm makes use of the superposition of local structural rearrangements for the description of conformational changes in the chains. The displacements of pairs of atoms subject to the geometrical constraints can be achieved in a computationally efficient way by the application of least-squares search methods. It is shown that a balance of the attractive interactions between the methylene chains and longer-range repulsive interactions between the charged headgroups determines the form of the spreading pressure isotherms. The experimental isotherms cannot be reproduced if the headgroups interact through purely repulsive potentials. We find it necessary either to modify these potentials by invoking a short-range attraction or to assume that the charge of a headgroup decreases with average area-per-molecule in the monolayers. Our model tracks the experimentally observed spreading pressure-area isotherm in Langmuir monolayers of ionised and non-ionised fatty acids. Importantly, we were able to reproduce the dependence of the isotherms on the chain length.

Keywords: Monte Carlo; flexibility; fatty acids; monolayers

This work was partly supported by the European Commission under TMR contract FMRX-CT97-0121 and by the Italian Ministry for Universities and Scientific and Technological Research (PRIN "Cristalli Liquidi").

INTRODUCTION

The numerical simulation of arrangements of amphiphilic molecules at water interfaces has attracted much research effort in recent years [1–22]. These molecules consist of flexible methylene chains attached to hydrophilic headgroups. The headgroups are localised at the water interface, which the methylene groups do not cross as a result of the so-called hydrophobic interactions.

The phase diagrams of Langmuir monolayers have been investigated for a long time from measurements of spreading pressure-molecular area (Π-a) isotherms at air-water interfaces [23,24]. Experiments have shown that unionised fatty acids and alcohols spread on water-air interfaces exhibit close-packed structures, while expanded assemblies are only formed on the ionisation of the carboxyl groups of the fatty acids. Nevertheless, saturated fatty acid chains containing more than 16 carbon atoms always form condensed monolayers at room temperature, while monolayers of myristic acid ($C_{14:0}$) exhibit a solid-liquid phase transition around 300 K [23,24]. It thus appears that the monolayer behaviour is determined by a balance between the attraction between the methylene groups of the chains and the repulsive interactions between the heads. While each chain contains a single site of repulsion, it possesses multiple sites of attraction, so that the behaviour of the monolayer will depend on the chain length of the constituent molecules.

The experimental observations have been summarized in terms of a generic phase diagram [24]. At low density (average area-per-chain, a, $>60\,\text{Å}^2$) the spreading pressure isotherms are characteristic of a 2-dimensional gaseous behaviour, as the inter-molecular interactions are negligible. Upon compression to areas-per-molecule of around 40–60 Å^2, a transition to the so-called liquid-expanded (LE) phase is encountered. Further compression of the system leads to the formation of a higher density phase, commonly known as the liquid-condensed (LC) phase, where the average area-per-chain is around 20 Å^2. If the LC phase of the monolayer is compressed even further, a continuous transition to a yet denser solid phase takes place, where the area-per-chain reaches a limiting value of 19 Å^2, characteristic of chains in their extended all-*trans* configuration.

The question as to which features of the amphiphilic molecules are essential in determining the phase diagram of Langmuir monolayers are conveniently addressed using computer simulations. While the balance between the repulsive interactions between the headgroups and the attractive interactions between the polymethylene chains is an important factor, the conformational degrees of freedom are also expected to play a crucial role.

The numerical simulation of assemblies of amphiphilic molecules is hampered not only by the complexity of the internal conformational motions but also by packing constraints. For this reason, a number of simplified models have been proposed for exploring the structure of the system [1,4,7,13,15,20,21,23]. The common feature of these approaches is the reduction of the monolayer structure to its rudiments, whereby the model chains are tethered to an impenetrable interface. A chain of spheres, each representing a functional group, either CH_2 or the headgroup, models the amphiphilic molecule. However, the coarse-grained representation, where methylene chains are represented as large spherical atoms connected by springs, with each model atom representing 2–3 CH_2 groups has attracted much attention [1,4,7,13,23]. Model systems were studied with constant volume (NVT) molecular dynamics methods [15,20,21], though isobaric (NPT) Monte Carlo methods have proved particularly successful.

These latter methods focus on local structural rearrangements and avoid dealing with restricted motions within conformational wells. The main challenge in this approach is the formulation of an efficient algorithm for changing the conformation of small chain segments. The general problem of implementing structural rearrangements in linear polymer chains was addressed by Gó and Scheraga [24]. Their ring-closure method is based on the observation that a segment of 4 bonded atoms with fixed ends can be displaced to new positions in an exact geometrical way, while conserving the bond lengths and valence angles. However, the practical implementation of the method is cumbersome and expensive in computer resources [25]. Recently, a number of improvements have been proposed, but under restricted conditions [26,27].

The numerically efficient coarse-grained representation has been widely used in recent years to investigate phase diagrams of model monolayers consisting of uncharged molecules. Here we shall extend these studies by addressing the question of balance between short-range attractive interchain interactions and the long-range repulsive headgroup interactions. To this end we present a new computational model with chemical group resolution. The model has been applied to investigations of the spreading pressure-area isotherms of Langmuir monolayers of fatty acids. The central premise of our model is that the conformational changes of a short chain arise from the superposition of random local structural rearrangements involving pairs of bonded atoms. However, as such moves cannot be accomplished within the framework of an analytical calculation, they were implemented using an optimising search algorithm. In doing this, we admit the possibility of small variations in bond lengths and valence angles of the model chains. While some computational efficiency is lost relative to the coarse-grained treatment, the algorithm is sufficiently fast to run on

individual workstations or PC's and monitor processes on a time scale long compared to the conformational changes of the polymethylene chains.

We show below that the experimental isotherms cannot be reproduced if the headgroups interact through purely repulsive potentials. We find it necessary either to modify these potentials by invoking a short-range attraction or to assume that the charge of a headgroup decreases with the average area-per-molecule in the monolayers. Our model tracks the experimentally observed spreading pressure-area isotherm in Langmuir monolayers of ionised and non-ionised fatty acids and reproduces the dependence of the isotherms on the chain length.

SIMULATION MODEL

Model Parameters

Each model surfactant chain consists of a linear sequence of $n-1$ methylene groups attached at one end to a hydrophilic headgroup. All the groups are treated as spherical united atoms, with diameters $\sigma_{CH} = 3.6\,\text{Å}$ for the methylene and terminal methyl groups and $\sigma_{HG} = 4.35\,\text{Å}$ for the headgroup. The bonds linking the n spherical atoms have a mean length d_0 of 1.54 Å, with a mean valence angle θ_0 of 109.47°. The torsional potential $V(\varphi)$ for the rotations about the C-C bonds of Toxvaerd [28] was used:

$$V(\varphi)/k_B = 972.9 + 1867.5\cos\varphi - 536.8\cos^2\varphi - 1856.3\cos^3\varphi + 1073.5\cos^4\varphi - 1520.8\cos^5\varphi \quad (1)$$

where k_B is the Boltzmann constant.

Methylene groups i and j either separated by more than 3 bonds along the same chain or on different chains were assumed to interact via the modified 6–12 Lennard-Jones potential:

$$V_{CC}(r_{ij})/k_B = 4\varepsilon_{CC}\left[\left(\frac{\sigma_{CH}}{r_{ij}}\right)^{12} - \left(\frac{\sigma_{CH}}{r_{ij}}\right)^{6}\right] + v_{ccc} \quad \text{for } r_{ij} \le 2.5\sigma_{CH} \quad (2)$$

where r_{ij} and σ_{CH} are the distance between the groups and their radius respectively, $\varepsilon_{CC} = 49\,\text{K}$ [15,19–21,29,30] and v_{ccc} is chosen so that V_{CC} is continuous at $2.5\,\sigma_{CH}$ and equal to 0. Note that here the terminal methyl and methylene groups of the chains are treated identically.

The repulsive interactions between the headgroups of chains i and j were described by a Debye screened Coulomb interaction potential [31,32]:

$$V_{HH}(r_{ij})/k_B = \left(\frac{\sigma_{HH}}{r_{ij}}\right)^{12} + \varepsilon_{HH}\frac{\exp(-\kappa r_{ij})}{r_{ij}} + v_{chh} \quad \text{for } r_{ij} \le 5\sigma_{HG} \quad (3)$$

where $\varepsilon_{HH} = q_i q_j / 4\pi\varepsilon\varepsilon_0$ and v_{chh} ensures that V_{HH} is continuous at $5\,\sigma_{HG}$ and equal to 0. On taking the dielectric permittivity ε to be 10 and each headgroup to be fully ionised, we find $\varepsilon_{HH} = 1.67 \times 10^4\,\mathrm{K}$.

The repulsive interactions between a headgroup and a methylene group either separated by more than 3 bonds on the same chain or on different chains were taken to be of the form:

$$V_{HC}(r_{ij})/k_B = \varepsilon_{HC}\left(\frac{\sigma_{HC}}{r_{ij}}\right)^9 + v_{chc} \quad \text{for } r_{ij} \le 2.5\sigma_{HC} \tag{4}$$

with $\sigma_{HC} = 1/2(\sigma_{CH} + \sigma_{HG})$, $\varepsilon_{HC} = 25\,\mathrm{K}$ and v_{chc} chosen so that V_{HC} is continuous at $2.5\,\sigma_{HC}$ and equal to 0.

The monolayer used in the simulations reported below was placed in a Monte Carlo box having a variable square cross-section in the xy-plane, with periodic boundary conditions. A linked-cell method [30] was implemented in the algorithm for the efficient evaluation of the inter-chain energies. Water molecules were not included. The headgroups (first atoms of the model lipid chains) were held near the local interface at $z = z_0$ using the asymmetric potential:

$$V_z/k_B = \begin{cases} 0 & \text{for } z \le z_0 \\ k_z(z - z_0)^2 & \text{for } z > z_0 \end{cases}. \tag{5}$$

The local interface was defined as the average position of the neighbouring headgroups along the z-axis. Consequently, the position of the interface varied slightly across the Monte Carlo box. We note that the half space $z \le z_0$ is the virtual water phase of the system.

Moreover, the effective methylene and terminal methyl groups were subjected to the repulsive harmonic potential $V_z/k_B = k_z(z - z_0)^2$ only on crossing the interface into the aqueous phase, $z \le z_0$. In this study we took $k_z = 1500\,\mathrm{K\,\AA^{-2}}$. We note that molecular dynamics simulations [20,21] employed a sharp sigmoid (step-like) tethering potential. The form of the latter potential is unsuited for a Monte-Carlo algorithm utilizing a Metropolis criterion. If any group happens to escape into the high-energy plateau, it will not incur any energetic penalties by moving even further away from the interface. This escape mechanism is blocked by the potential used here.

Conformational Moves

The conformational dynamics of the model hydrocarbon chain were assumed to arise from a superposition of local structural arrangements involving the simultaneous move of a pair of adjacent atoms, -C_j-C_{j+1}-, to different positions in space. Essentially, the pair of atoms to be moved is chosen at random and each is given a random displacement. The displacement of atom C_j is effected by a random rotation about bond $j-2$,

joining atoms C_{j-2} and C_{j-1}, while atom C_{j+1} is displaced by a random rotation about bond $j+2$ joining atoms C_{j+2} and C_{j+3}. The move thus involves two angular variables. The final positions of the two atoms are found on searching the solution space using either a Marquardt-Levenburg or a Conjugate Gradients least-squares algorithm [33] by minimising the energy functional f

$$f = |\vec{r}_{j+1} - \vec{r}_j|^2 + \sum_{i=j}^{j+1} (\cos\theta_i - \cos\theta_0)^2 \tag{6}$$

where θ_j is the valence angle at atom j and $\vec{r}_j$ its the position vector. For pairs of atoms away from the ends of the chains this implies that 2 torsional angle variables are optimised in a least-squares sense so as to reduce χ^2 using 3 constraints. In order to implement the same moves at the ends of the chains, i.e. for the pairs of atoms {2,3} and $\{n-2, n-1\}$, we have introduced two phantom atoms 0 and $n+1$. These two phantom atoms, as well as the two terminal atoms *1* and n are moved individually by carrying out a random rotation about the end bonds. We note that this algorithm is applicable to both saturated chains and chains containing unsaturated segments. A double bond in the chain can be introduced by the simple stratagem of imposing a strong torsional potential around that bond.

The new coordinates of the pair of moved atoms are now used to calculate the total energy, $U_{total} = V(\varphi) + V_{CC} + V_{HH} + V_{HC}$. Note that the energies corresponding to the bond length and valence angles are omitted. The move is accepted subject to the usual Metropolis criterion: $\exp(-\Delta U/T) > \eta$, where $0 < \eta < 1$ is a random number and ΔU is the difference between the old and the new total energies.

Constant Pressure Algorithm

The Monte Carlo algorithm for a system containing N model chains each consisting of n atoms at a given spreading pressure Π and temperature T, was executed in the following way. Given a particular configuration of the monolayer, Ω_j, the local conformational moves described above are attempted $N \times n$ times with the Metropolis criterion applied after each attempt. If a local move is rejected, the old co-ordinates of the atoms involved are retained. These moves generate a new configuration of the monolayer, Ω_{j+1}. The cycle is now repeated using Ω_{j+1} as the starting configuration. Every 5 moves, the area of the square Monte Carlo box was changed at random by a maximum of $\Delta A = \pm 0.1\,\text{Å}^2$. The positions of the headgroups in the box were scaled accordingly and the model chains were rebuilt from their known bond vectors. In this way whole-body translational moves of the chains were accomplished. These trial moves

were accepted or rejected with the Metropolis criterion using the effective free energy [3,30] F:

$$F = E + \Pi A - NTk_B \ln\{A\} \tag{7}$$

where $E = V_{CC} + V_{HH} + V_{HC}$ is the *inter-chain* energy, Π the applied spreading pressure and A the area of the simulation box. The spreading pressures used varied between 2 and 20 dynes/cm, a range corresponding to that used in experiments.

The monolayers consisted typically of 1024 model chains 14 atoms long. The simulation started from an assembly of chains in their all-*trans* conformation and the equilibrium area at a given spreading pressure was reached after generating about 20,000 monolayer configurations. The system was then observed for a further 10,000 monolayer configurations. All the simulations were carried out at 300 K. We found it useful, see discussion below, to split the simulation runs into cycles of 500 configurations. Each cycle consisted of a run of 50 configurations at a constant box size with the inter-chain interactions switched off, followed by a run of 450 simulations with the inter-chain interactions active.

RESULTS AND DISCUSSION

A Geometrical Validation of the Algorithm

One of the challenges in simulations of large molecules, be they linear or closed rings, is the formulation of an efficient algorithm for changing the conformation of small segments. Mostly, the algorithms used are variants of the ring-closure method proposed by Gó and Scheraga [24]. This latter method is based on the observation that a segment of 4 bonded atoms with fixed ends can be displaced to new positions in an exact geometrical way, while conserving the bond lengths and valence angles. However, the numerical implementation of the method is cumbersome and expensive in computer resources. It was applied for instance to Monte Carlo simulations of polymer systems [25], but proved to be very time consuming. There have been recent reports of improved implementations, but always under restricted conditions [26,27]. Here we note that besides the numerical inefficiency of such an exact concerted move algorithm, the moves executed involve large-scale conformational changes in chains consisting of 12–20 atoms and will be suppressed significantly in a close-packed system. For these reasons we have developed a more appropriate algorithm for the simulations of short chained molecules. The working hypothesis of our model is that the conformational changes of a short chain arise from the superposition of random local structural rearrangements involving pairs of bonded atoms. While it is an easy matter to formulate an analytical

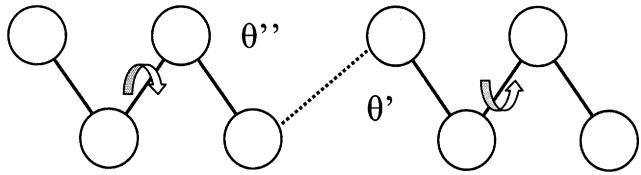

FIGURE 1 Schematic representation of the local conformational moves. The dashed line denotes the central bond whose length is adjusted by the search algorithm. The values of the two valence angles θ' and θ'' are adjusted simultaneously.

algorithm for moves that preserve the bond length [34], this is not the case for the valence angles. We have therefore admitted the possibility of valence angles varying by up to 20° about the pre-set mean angle θ_0.

The local conformational changes are implemented through random changes in two torsional angles, each chosen at random in the uniform interval [−180°, 180°]. We have chosen these driver angles to be at the ends of the moving segment, so that each one moves a single atom, see Figure 1. For instance, a random rotation about bond $j-2$, joining atoms C_{j-2} and C_{j-1} displaces atom C_j. Each atom C_j and C_{j+1} thus describes a circular path in space. The relative orientation and separation of the circles depend on the spatial positions of bonds $j-2$ and $j+2$, or in other words by the conformation of the chain. As a consequence of the moves, both the length of the bond joining the moving atoms, as well as the two valence angles between the three bond vectors attached to these atoms are modified.

New positions for the atoms consistent with the geometrical structure of the chain cannot be described in closed form. Rather, they need to be found by a search through the solution space with an optimising algorithm. Here we search for those values of the bond length and two valence angles, which minimise the energy functional f, Eq. (6). We have applied this formalism using two search algorithms, one employing the classical non-linear Marquardt-Levenburg method and one based on a Conjugate-Gradient approach. Both these methods prove to be numerically efficient and produce highly peaked distributions of valence angles about the mean value of 109.47°. The distribution of the valence angle about bond 6 at the centre of an isolated chain of 14 atoms is shown in Figure 2. Identical distributions are found for all bonds in the chain and they turn out to be independent of the chain length. It can be seen from the distribution that over 95% of the valence angles lie within $\pm 5°$ of the pre-set mean value. The distribution of bond lengths obtained is equally sharp, see Figure 3. Moreover, we find that the results are the same for every starting conformation, including the *all-trans* chain.

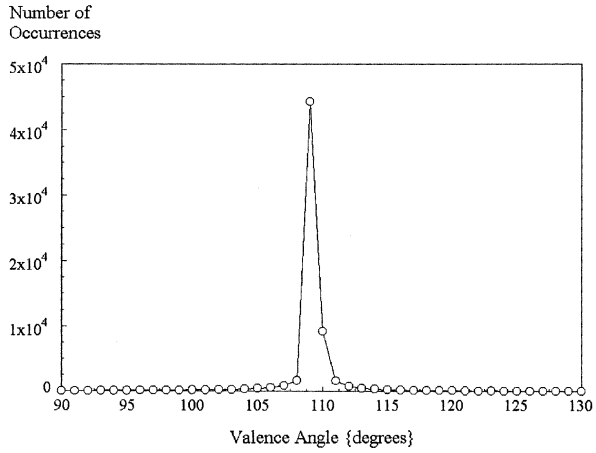

FIGURE 2 Distribution of the valence angle between bonds 6 and 7 at the centre of a free 14-atom model chain obtained from the simulations.

The Marquardt-Levenburg search procedure is some 30% faster than the Conjugate-Gradient approach in producing a trajectory of a given number of chain conformations. However, the acceptance rate of the latter algorithm is about 20% higher than that of the former. Other optimising algorithms produce satisfactory results, but appear to be less efficient numerically. The usefulness of the algorithm lies primarily in its implementation of a variable step size in the search procedure.

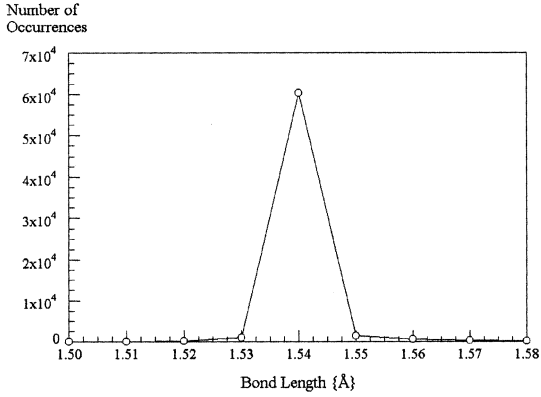

FIGURE 3 Distribution of the length of bond 6 at the centre of a free 14-atom model chain obtained from the simulations.

These results demonstrate that our algorithm produces chain conformations consistent with the expected rigid geometrical structure. It now remains to show that the algorithm samples the space of torsional angles correctly.

Torsional Angle Space

We note that while only two atoms change their positions in space, the torsional angles about five bonds are affected by the move, see Figure 1. This arises because the orientation of bond l defines the torsional angles about bonds $l-1$ and $l+1$ and here three bonds, $j-1$, j and $j+1$ are moved. The question now arises whether the local moves implemented in the model span all the torsional angles for the C-C bonds. In particular, the algorithm should provide a uniform mapping between the driver angles and the space of internal torsional angles characterizing the conformation of a chain. To this end we performed simulations on a single chain subjected only to the geometrical constraints of the search algorithm.

The torsional angle distribution, $J(\varphi)$, is found to be bimodal about the *trans* ($\varphi = 180°$) position, with sharp peaks at the trans and *cis* positions for all the internal bonds of the chain, Figure 4. The corresponding distribution for the two terminal bonds is, however, flatter between the *trans* and *cis* positions. The distribution $J(\varphi)$ obtained with the Conjugate-Gradient algorithm, Figure 4, was found to be smoother than that yielded by the Marquardt-Levenburg approach. For this reason we decided to use the former method in our simulations. A uniform distribution

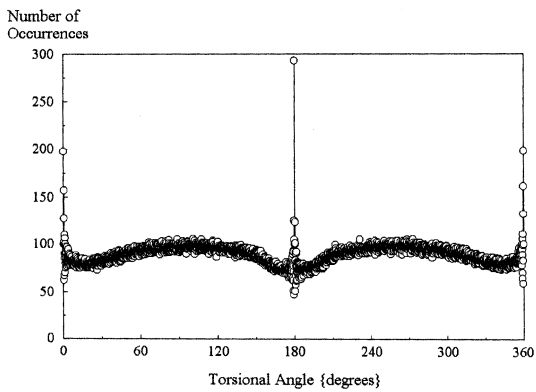

FIGURE 4 Torsional angle distribution about bond 6 of a free 14-atom model chain yielded by the two-atom moves of the algorithm.

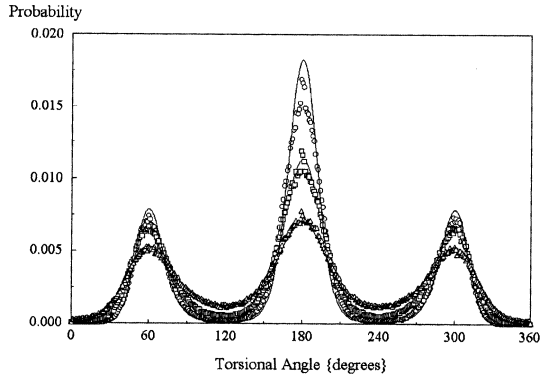

FIGURE 5 Torsional angle distribution about bond 6 of a free chain of 14 point atoms subjected to the torsional potential, Eq. (1) at 300 K, 500 K and 900 K. The continuous lines give the Boltzmann distribution at the corresponding temperature.

of torsional angles can be recovered simply by weighting the acceptance rate by the ratio $\prod_{i=j-2}^{j+2} J(\varphi_{old,i}) / \prod_{i=j-2}^{j+2} J(\varphi_{new,i})$. The raw distributions, $J(\varphi)$, obtained from the simulations are used for the weighting in the simulations.

As a further check of the method, we now subject each bond of the chain to the torsional potential $V(\varphi)$ of Eq. (1). The distributions of the torsional angles obtained are in good agreement with a Boltzmann distribution over $V(\varphi)$ at the appropriate temperature, see Figure 5. We note that the comparison between the simulation data and the Boltzmann distribution is direct, since temperature is the only parameter.

Our findings thus provide a clear indication that the model presented here closely mimics the conformational behaviour of realistic polymethylene chains.

Detailed Balance

As the last check of our algorithm, we shall address the question as to whether the requirement of microscopic reversibility, or detailed balance, is satisfied. The application of the Metropolis criterion in a Monte Carlo algorithm can only be justified if this condition is met. Unfortunately, the use of an optimising algorithm for the implementation of moves in our algorithm precludes a formal proof that this is indeed the case.

It can thus be argued that the algorithm presented above does not sample the configuration space of the chains in a way leading to a correct Boltzmann distribution over the internal degrees of freedom, the bond lengths and valence angles. A full discussion of this difficulty will be

deferred to a following paper. Here, we shall simply resort to consistency arguments using the numerical data obtained from the simulations.

In the first place, we note that the distributions of bond lengths and valence angles should be independent of temperature, in view of the high energies involved. It is easy to show that the corresponding energy functional, Eq. (6), has a single and distinct global solution basin with $f < 0.01$. The basin contains 2 to 4 local minima separated by low energy barriers. It represents a solution region where the bond length deviates by no more than 0.04 Å from its equilibrium value of 1.54 Å and the valence angles assume values within 20° of the pre-set mean value. Other solution basins, corresponding to much larger deviations from the pre-set values are always present, but these lie at much higher values (> 5) of the functional f. The distributions of valence angles and bond lengths found in the simulations, see Figures 2 and 3, indicate that the optimising algorithm searches only the global solution basin. We have shown previously [35] that during a simulation run the algorithm finds the local minima with a probability proportional to their Boltzmann weights.

In the second place, marked deviations from the condition of detailed balance will become apparent when sampling the space of torsional conformations of the chains. We thus expect an incorrect algorithm to produce a distorted (i.e. non-Boltzmann) distribution of torsional angles about any bond of the chain, but particularly so at its centre. Moreover, the auto-correlation functions of the spatial orientation of bond vectors along a trajectory will not exhibit a monotonous decay to zero.

Simulations of chains of point atoms at different temperatures show that the algorithm yields distributions of torsional angles corresponding to the appropriate Boltzmann distribution over $V(\varphi)$, see Figure 5.

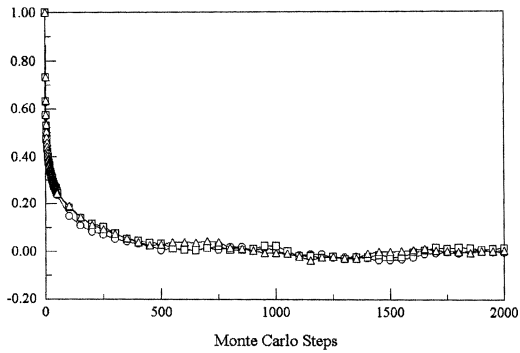

FIGURE 6 The auto-correlation function $G_j(m) = \langle \vec{b}_j[n] \cdot \vec{b}_j[n+m] \rangle$ for bond vectors $j = 7$ and 10, near the centre of a free chain of 16 point atoms.

Moreover, the autocorrelation function for every bond vector j, $G_j(m) = \langle \vec{b}_j[n] \cdot \vec{b}_j[n+m] \rangle$, decays to zero smoothly as expected, see Figure 6. Here $\vec{b}_j$ [l] denotes the bond vector for chain conformation l and $\langle \cdots \rangle$ denotes an average along the trajectory.

The findings above provide strong evidence for the view that the algorithm presented here satisfies the requirement of detailed balance.

Choice of Model Parameters

The guiding principle in choosing values for the parameters characterising the strength of the potentials, is the experimental observation that the monolayer behaviour is determined by a balance between the attraction between the methylene groups of the chains and the repulsive interactions between the heads. It is moreover evident that each chain contains a single site of repulsion, but multiple sites of attraction, so that the behaviour of the monolayer will depend on the chain length of the constituent molecules. Experiments have shown that unionised fatty acids and alcohols spread on water-air interfaces exhibit close-packed monolayers, while expanded assemblies are only formed on the ionisation of the carboxyl groups of the fatty acids. Nevertheless, saturated fatty acid chains containing more than 16 carbon atoms always form condensed monolayers at room temperature, while monolayers of myristic acid ($C_{14:0}$) exhibit a solid-liquid phase transition around 300 K [23,24]. It is for this latter reason that we have chosen to explore the behaviour of a model monolayer consisting of 14 atomic groups.

The starting point for the simulation was the characterization of the screening constant κ appearing in the screened Debye potential of the headgroup-headgroup interactions [31,32] The value of this parameter is strongly correlated with our choice for the effective relative dielectric constant characterizing the interactions between the headgroups and that for ε_{CC}, determining the attractive interactions between the methylene groups. We have used the generally accepted value of 49 K for the latter parameter and set the relative dielectric permittivity at 10. We have found that a lower value for the effective permittivity, leading to a stronger repulsive interaction, can be compensated by increasing the screening of the charges through a higher value of κ. It is clear that weaker attractive interactions between the methylene groups can be balanced by weaker repulsive potentials, produced for instance by a higher degree of screening of the headgroups.

In order to determine the value of κ, we carried out constant pressure simulations of monolayers of model myristic acid chains at a spreading pressure of 2.5 dyne/cm and 300 K. As the value of κ decreased, the repulsive interactions between the headgroups increased, because of a

reduced degree of screening. The change in the screening constant κ was carried out systematically in order to reproduce the experimentally observed area-per-molecule of around $36\,\text{Å}^2$. The other interactions, see above, were kept constant throughout.

The simulations showed that for $\kappa > 0.24\,\text{Å}^{-1}$ (a high screening efficiency resulting in weaker repulsive interactions), the monolayers collapsed to the liquid-condensed state when the initial area-per-molecule, a, was greater than $22\,\text{Å}^2$. If the starting area-per-molecule was chosen to be close to the cross-sectional area of the all-*trans* configuration, $19\,\text{Å}^2$, the monolayer did not expand during the simulation run. These observations are in good agreement with experiments on uncharged fatty acid monolayers [23,24].

An area-per-molecule of $41.3\,\text{Å}^2$ was found on taking $\kappa = 0.18\,\text{Å}^{-1}$. This potential can be approximated with an r^{-3} distance dependence for $r > 6\,\text{Å}$. However, on increasing the spreading pressure to 20 dynes/cm, the area decreased to only $36.6\,\text{Å}^2$, Figure 7. A further reduction in the area-per-molecule was only realised on increasing the surface pressures to over 60 dynes/cm. These findings are at odds with experimental observations.

In our simulations we have taken the inter-group interactions to be determined by their centre-to-centre distances. The question now arises as to whether an anisotropic interaction, with the sites of the interaction displaced relative to the geometric centre of the group, will alleviate the situation. Such anisotropic potentials have been studied in great detail in simulations of the thermodynamic and transport properties of liquid hydrocarbons [20,21,29]. We have found that in our case, the incorporation of such potentials does not produce any essential changes in the spreading pressure isotherms. It is the strength of the interactions between the methylene groups rather than their anisotropy that affects the simulation results.

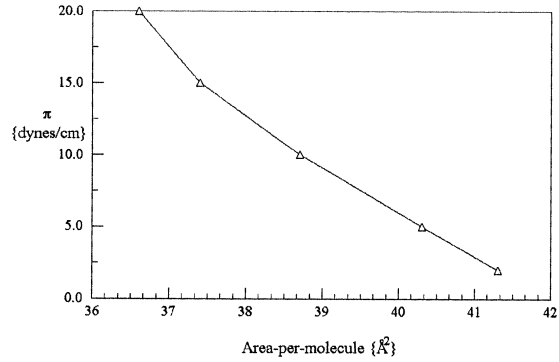

FIGURE 7 Spreading pressure-area isotherm simulated at 300 K for a model monolayer consisting of 14-atom chains with charged headgroups.

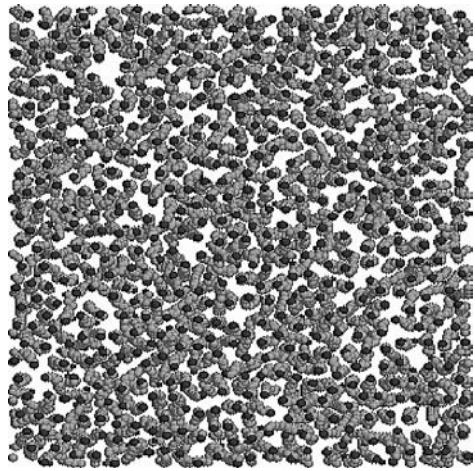

FIGURE 8 An in-plane view of a model monolayer at an area-per-molecule of 41.3 $Å^2$ at 300 K. The headgroups of the chains are denoted by a darker shade of grey.

Simulations using a value of 12 K for ε_{CC}, instead of the literature value of around 49 K, were found by us to track the experimentally observed thermal isotherms, albeit with a significantly higher value of κ [35]. This clearly indicates that a fine balance between the repulsive headgroup-headgroup interactions and the attractive interactions between the methylene groups determines the monolayer behaviour. In particular we conclude that the strong repulsions between the headgroups needed to balance the inter-chain attractions, lead to the formation of fairly incompressible monolayers. We have found furthermore, that the attractive interactions suppress the translational diffusion of the fatty acid chains over the surface of the monolayer. In fact the in-plane structure of the monolayer is inhomogeneous, with the chains tending to form dynamic clusters at areas-per-molecule above 22 $Å^2$, see Figure 8. In view of the lack of in-plane translational diffusion, we implemented the cyclic algorithm described above, where the interactions between groups are switched off at regular intervals to allow the clusters to reform.

Formulation of the Effective Headgroup-Headgroup Repulsive Potential

It is clear that the repulsive potential needs to be modified in order to reproduce a condensed monolayer structure at spreading pressures in the range 20 dynes/cm–30 dynes/cm. The modification of the effective potential should ideally reflect the effects of the aqueous substrate, for instance through an electric double layer, on the headgroup interactions. Our

simulations show that a realistic effective potential must moderate the sharp rise of the Debye potential at short inter-headgroup distances.

We shall now consider two possible mechanisms leading to a moderation of the repulsive potential between the charged headgroups. In the first place, we note that the carboxyl groups on the chains are weak acids and may not necessarily be fully ionised. This behaviour can be modelled simply by assuming that the monolayer consists of a mixture of fully ionised, $q = 1$, and unionised, $q = 0$, molecules and is characterized by its average charge, $\langle q \rangle$. Here we denote the charge in units of the elementary charge of an electron, e. The screening constant was kept at $\kappa = 0.22\,\text{Å}^{-1}$ The simulations show that an area-per-molecule in the range $37\,\text{Å}^2$ to $41\,\text{Å}^2$ at a spreading pressure of 2.5 dynes/cm can be obtained with $\langle q \rangle$ in the range $1.0e$ to $0.95e$. However, areas-per-molecule of around $23\,\text{Å}^2$ at a spreading pressure of 20 dynes/cm are only found on reducing $\langle q \rangle$ to less than $0.75e$. A more complex charge distribution corresponding to a particular value of $\langle q \rangle$ may be generated using the Maximum Entropy Model, i.e. $f(q) = exp(\lambda_0 + \lambda_1 q)$. Here the value of λ_0 is obtained from the normalization condition and λ_1 is chosen so as to reproduce the preset value of $\langle q \rangle$. The value of q assigned to a particular headgroup is now given by $q = \ln\{1. + \eta[\exp(\lambda_1) - 1.]\}/\lambda_1$, where $0 \leq \eta \leq 1$ is a random number denoting the probability that the headgroup will acquire a charge between 0 and q. As in the case of the binary model above, areas-per-molecule less than $23\,\text{Å}^2$ at a spreading pressure of 20 dynes/cm are found with values of $\langle q \rangle$ less than $0.8e$.

This indicates that the simulations will reproduce the pressure isotherms if the effective repulsive interactions between the headgroups are a decreasing function of the area-per-molecule. A simple implementation of such a potential in the spirit of the united atom description, is accomplished on taking the charge of a headgroup q_i, to be a function of average-area-per-molecule, a: $q_i(a) = e\{1. - \exp[-\alpha(a - 18)]\}$. This implies that the expression incorporates all the changes in the electrostatic energies of the headgroups as the charge varies.

A second modification of the Debye potential can be implemented on invoking *ad-hoc* the presence of a short-range attractive potential. This potential may be attributed to the mediation of the electrostatics interaction between the headgroups by the aqueous substrate, which has been neglected in the simulations. We shall here only consider a generic contribution from dipolar interactions of the form:

$$V'_{HH}(r_{ij})/k_B = -\varepsilon'_{HH}\left(\frac{\sigma'_{HH}}{r_{ij}}\right)^6 \tag{8}$$

and choose the values of ε'_{HH} and σ'_{HH} so as to reproduce the experimental spreading pressure isotherms for a given value of κ. Typical forms of the

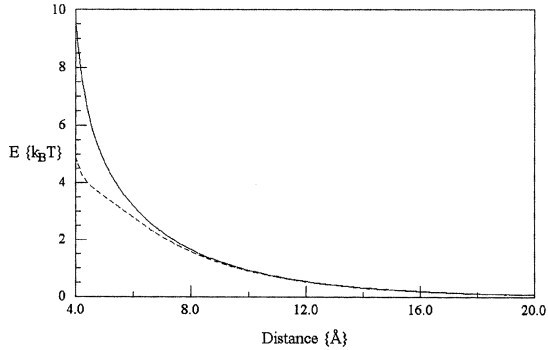

FIGURE 9 The repulsive Debye potential, $\kappa = 0.18\,\text{Å}^{-1}$, and the modification introduced by the a short-range attractive potential, Eq. (8) with $\varepsilon'_{HH} = 0.05\,\varepsilon'_{HH}$.

total potential, $V_{HH} + V'_{HH}$ is shown in Figure 9. The figure shows that the dipolar contribution moderates the rise in the repulsive interactions primarily at distances in the range $0.8\sigma_{HG} \leq r_{ij} \leq 1.2\sigma_{HG}$ for $0 \leq \varepsilon'_{HH} \leq 0.08\varepsilon_{HH}$.We note that the value of κ will be somewhat smaller than in the case of a variable headgroup charge. An area-per-molecule of $39.5\,\text{Å}^2$ at 2.5 dynes/cm was found on taking $\varepsilon'_{HH} = 0.04\varepsilon_{HH}$ with $\sigma'_{HG} = \sigma_{HG}$ and $\kappa = 0.18\,\text{Å}^{-1}$. However, the area-per-molecule decreases to only $28.5\,\text{Å}^2$ on increasing the spreading pressure to 20 dynes/cm. This finding indicates again that an area-dependent contribution is needed to reproduce the experimental isotherms.

Constant Pressure Simulations

We shall here illustrate the area-dependent effects for the simple variable charge model in simulations of the spreading pressure isotherms of monolayers of myristic acid at 300 K. To this end we have used the combination $\alpha = 0.2$ and $\kappa = 0.22\,\text{Å}^{-1}$ and the results are shown in Figure 10. The figure shows that the simulations reproduce the principal features of the experimentally observed spreading pressure isotherms. In particular, the simulated isotherms show that the monolayer collapses to a condensed structure at spreading pressures above 7.5 dynes/cm. This collapse is indicative of a phase transition, as expected experimentally. We have found that the simulations in the spreading pressure interval 7.5 dynes/cm–10 dynes/cm were susceptible to fluctuations, so that the isotherms could not be tracked with confidence. Also shown in Figure 10, are the corresponding isotherms for model lauric acid ($C_{12:0}$) chains, using the same model parameters. These exhibit the characteristic of a liquid

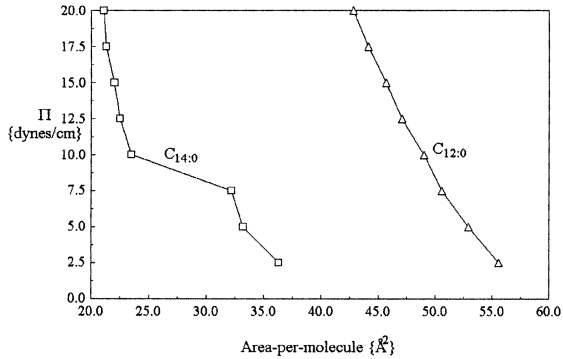

FIGURE 10 Spreading pressure-area isotherms of model monolayers obtained from the simulations at 300 K: myristic acid chains, $C_{14:0}$; Δ lauric acid chains, $C_{12:0}$.

monolayer far from a phase transition. In contrast, model palmitic acid ($C_{16:0}$) chains are found to form a condensed monolayer at all spreading pressures. Similar results are obtained on introducing the short-range attractive potential, Eq. (8). However, now it is necessary to assume that ε'_{HH} varies linearly with the applied spreading pressure. These results show that the simulation method described here tracks the effect of chain length on the phase of a monolayer as observed experimentally. The proviso being that the effective potential for the repulsive headgroup interactions varies with the area-per-molecule in the monolayer structure.

CONCLUSIONS

We have presented above a new off-lattice Monte Carlo algorithm for simulating the conformational behaviour of surfactant soap molecules tethered to a planar interface. The extension to other geometrical arrangements is straightforward. The algorithm makes use of the superposition of local structural rearrangements for the description of conformational changes in the chains. The displacements of pairs of atoms subject to the geometrical constraints can be achieved in a computationally efficient way by the application of least-squares search methods.

It is shown that a balance of the attractive interactions between the methylene chains and longer-range repulsive interactions between the charged headgroups determines the form of the spreading pressure isotherms. The experimental isotherms cannot be reproduced if the headgroups interact through purely repulsive potentials. We find it necessary either to modify these potentials either by invoking an area-dependent

short-range attraction or by assuming that the charge of a headgroup decreases with average area-per-molecule in the monolayers. Our model tracks the experimentally observed spreading pressure-area isotherm in Langmuir monolayers of ionised and un-ionised fatty acids. Importantly, we were able to reproduce the dependence of the isotherms on the chain length.

Finally we note, that the algorithm presented here can be extended in a straightforward way to simulations of any molecule consisting of a flexible chain attached to a (semi)rigid core such as cyanobiphenyls or cholesterol.

REFERENCES

[1] Opps, S. B., Yang, B., Gray, C. G., & Sullivan, D. E. (2001). *Phys. Rev. E*, *63*, 1063.
[2] Fujiwara, S. & Sato, T. (1999). *J. Chem. Phys.*, *110*, 9757.
[3] Stadler, C., Lange, H., & Schmid, F. (1999). *Phys. Rev. E*, *59*, 4248.
[4] Goetz, R. & Lipowsky, R. (1998). *J. Chem. Phys.*, *108*, 7397.
[5] von Gottberg, F. K., Smith, K. A., & Hatton, T. A., (1997). *J. Chem. Phys.*, *106*, 9850.
[6] Mackie, A. D., Panagiotopoulos, A. Z., & Szleifer, I. (1997). *Langmuir*, *13*, 5022.
[7] Schmid, F. & Lange, H. (1997). *J. Chem. Phys.*, *106*, 3757.
[8] Shinoda, W., Namiki, N., & Okazaki, S. (1997). *J. Chem. Phys.*, *106*, 5731.
[9] Desplat, J.-C. & Care, C. M. (1996). *Molec. Phys.*, *87*, 441.
[10] Palmer, B. J. & Liu, J. (1996). *Langmuir*, *12*, 746.
[11] Tieleman, D. P. & Berendsen, H., J. C. (1996). *J. Chem. Phys.*, *105*, 4871.
[12] Zhang, Z., Davis, H. T. & Kroll, D. M. (1996). *Phys. Rev. E*, *53*, 1422.
[13] Haas, F. M., Hilfer, R. & Binder, K. (1995). *J. Chem. Phys.*, *102*, 2960.
[14] Tu, K., Tobias, D. J. & Klein, M. L. (1995). *Biophys. J.*, *69*, 2558.
[15] Xiang, T.-X. & Anderson, B. D. (1995). *J. Chem. Phys.*, *103*, 8666.
[16] Rector, D. R., van Swol, F., & Henderson, J. R. (1994). *Molec. Phys.*, *82*, 1009.
[17] Bassolino-Klimas, D., Alper, H. E., & Stouch, T. R. (1993). *Biochemistry*, *32*, 12624.
[18] Heller, H., Schaefer, M., & Schulten, K. (1993). *J. Phys. Chem.*, *97*, 8343.
[19] Smit, B., Esselink, K., Hilbers, P. A. J., van Os, N. M., Rupert, L. A. M., & Szleifer, I. (1993). *Langmuir*, *9*, 9.
[20] Karaborni, S. & Toxvaerd, S. (1992). *J. Chem. Phys.*, *96*, 5505.
[21] Karaboni, S., Toxvaerd, S., & Olsen, H. (1992). *J. Phys. Chem.*, *96*, 4965.
[22] Moller, M. A., Tildesley, D. J., & Kim, K. S. (1991). *J. Chem. Phys.*, *91*, 8390.
[23] Adam, N. K. (1938). *The physics and chemistry of surfaces*, Clarendon Press: Oxford.
[24] Gaines, G. L., Jr. (1996). *Insoluble monolayers at gas- liquid interfaces*, Interscience Publishers: New York.
[25] Sintes, T. & Baumgärtner, A. (1997). *Biophys. J.*, *73*, 2251.
[26] Gõ, N. & Scheraga, H. A. (1970). *Macromolecules*, *3*, 178.
[27] Dodd, L. R., Boone, T. D., & Theodorou, D. N. (1993). *Molec. Phys.*, *78*, 961.
[28] Favrin, G., Irbäck, A., & Sjunnesson, F. (2001). *J. Chem. Phys.*, *114*, 8154.
[29] Chen, Z. & Escobedo, F. A. (2000). *J. Chem. Phys.*, *113*, 11382.
[30] Toxvaerd, S. (1988). *J. Chem. Phys.*, *89*, 3808.
[31] Ungerer, P., Beauvais, C., Delhommelle, J., Boutin, A., Rousseau, B., & Fuchs, A. H. (2000). *J. Chem. Phys.*, *112*, 5499.
[32] Frenkel, D. & Smit, B. (1996). *Understanding molecular simulation*, Academic Press: San Diego.
[33] Landau, L. D. & Lifshitz, E. M. (1959). *Statistical mechanics*, Pergamon Press: London, chapter 7.

[34] Israelachvili, J. N. (1985). ***Intermolecular and surface forces***, Academic Press: London.
[35] Press, W. H., Teukolsky, S. A., Vettering, W. T., & Flannery, B. P. (1992). ***Numerical Recipes in Fortran***, Cambridge University Press, New York.
[36] Li, X.-J. & Chiew, Y. C. (1994). ***J. Chem. Phys.***, ***101***, 2522.
[37] Polimeno, A., Ros, J. M., & Levine, Y. K. (2001). ***J. Chem. Phys.***, ***115***, 6185.